

Simple Realization of Integral Fuzzy Control for Isolated AHPFC Converters^{*}

Kuang-Yow Lian^{*} and Chi-Wang Hong^{**}

^{*} National Taipei University of Technology, Taipei 10608, Taiwan (Tel: 886-2-27712171 # 2171; email: kylian@ntut.edu.tw)

^{**} Chung-Yuan Christian University, Chung-Li 32023, Taiwan (Tel: 886-3-2654822; e-mail: chiwang@cycu.edu.tw)

Abstract: This paper proposes an integral Takagi-Sugeno (T-S) fuzzy controller to achieve the output voltage regulation for an AC-DC isolated active high power factor correction (AHPFC) converter. The converter can avoid high voltage stresses and decrease harmonic distortions under discontinuous conduction mode (DCM). The dynamics of the converter are derived by the AM-TTS-DS method. To ensure zero steady-state error, we add an extra integral error signal to the dynamics. Translating coordinate to the DC operating points, the converter's stabilization model can be determined. Both feedback gains and system stability are inferred simultaneously. The control gains can be obtained by solving linear matrix inequalities (LMIs) via Matlab's toolbox. A surprising property is that the obtained feedback gains are identical for every fuzzy control rule. This condition greatly simplifies the realization using analog circuits. The simulations and experimental results exhibit the satisfactory performance of the converter with the designed integral T-S fuzzy regulator.

1. INTRODUCTION

Presently, AC/DC power factor correction (PFC) converters have two major categories: cascade two-stage topology and integrated single-stage one. The two-stage bears from high cost and complex circuit. On the other hand, the single-stage is provided with effective cost and simpler circuit, but it has some drawbacks such as high voltage spike and component stress. As a novel single-stage topology, the isolated active-high-power-factor-correction (AHPFC) converter, combined a PFC and a regulator would actively force a line current to follow an applied sinusoidal waveform voltage, see Lin et al. [2005]. Under operating in discontinuous conduction mode (DCM), both the PFC cell implemented by a buck-boost converter and the regulator cell performed by a flyback converter can provide the inherent power factor correction and resolve the high voltage stress of the bulk capacitor, relatively. Due to this AHPFC converter employs only one controller with one switch, the control strategies become very important for holding such essential properties.

In the past years, the linear control system was designed for many power converters, including the above mentioned AHPFC. However, the transfer functions from input voltage to output voltage and from duty ratio to output must be calculated by very multifarious processes in classical control fields. The proportional integral (PI) controller provides only few feedback gains to regulate the PWM signals, that difficultly govern the internal nonlinear states' variations of the converters, see Kanaan et al. [2004]. Consequently, the traditional Mamdani-type fuzzy approach is suggested to control some converters for achieving nice-

performance, see Viswanathan et al. [2005]. In addition, the fuzzy logic controller (FLC) has been extensively designed for the higher nonlinear PFC converters, but most researches are limited on boost-type PFC, see Kirawanich et al. [2004]. Moreover, the stability of the traditional fuzzy system has not been analyzed theoretically in a specific way.

Compared to the traditional fuzzy methods, the stability of the Takagi-Sugeno (T-S) fuzzy model-based approach can be rigorously proven by Lyapunov theorem. Significantly, the linear matrix inequality (LMI) formulation can powerfully reduce both the stability analysis and the control design issues for a T-S fuzzy modelling system, see Tanaka et al. [2000]. Since the integral control is usually used to achieve zero steady-state error for the constant disturbances of physical dynamic systems, so that the LMI-based integral T-S fuzzy schemes are proposed to control the DC-DC buck converter, see Lian et al. [2006]. But it had never been used on the AC-DC isolated PFC converters.

This paper proposes an integral T-S fuzzy model-based controller to resolve the highly nonlinear character of AC-DC AHPFC converter. First, for reflecting the system's fast and slow time variables, we derive the dynamics of the converter by using the average method called two-time-scale discontinuous system (AM-TTS-DS), see Sun et al. [1992]. Next, we offer the integral T-S fuzzy method to model the AHPFC converter with an emphasis on addressing its nonlinear terms. The system's exponential stability is proven by Lyapunov theorem and the control gains are obtained via Matlab's toolbox. Since this converter system has two nonlinear terms and three states (including an integral error), there are twelve control gains to act in responsibility to tune the duty ratio of the switch.

^{*} This work was supported by the National Science Council, R.O.C, under Grant NSC-94-2213-E-033-004.

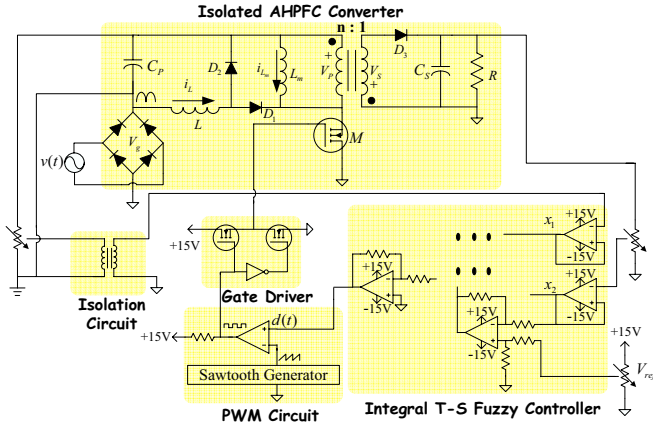


Fig. 1. Closed-loop structure of isolated AHPFC converter.

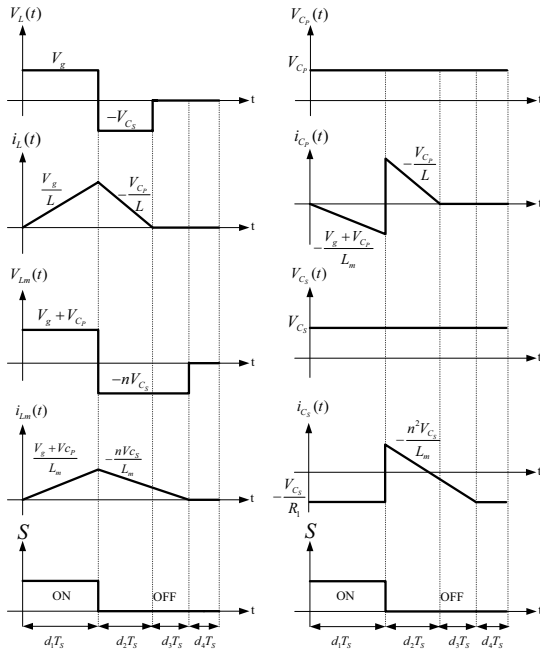


Fig. 2. Ideal waveforms on inductors and capacitors.

The proposed approach would further intensify the control potency for other converters than using linear methods. Finally, the performances of converter are confirmed by numerical simulation and hardware experiments.

2. DYNAMICS OF ISOLATED AHPFC CONVERTER

Fig. 1 shows an AC-DC isolated AHPFC converter with an integral T-S fuzzy controller, which is designed and implemented by electronic circuits. Here, M denotes a power switch MOSFET. The converter's operating principle is described with assumptions: (i) under steady-state conditions; (ii) ideal switching components; and (iii) C_P and C_S are large enough, hence a constant voltage can be across it. Thus, the analytical procedure can be divided into four stages relative to four subinterval ($d_1T_S \sim d_4T_S$) in one switching period (T_S) as follows. Stage 1 (M :on, D_1 :on, D_2 :off, D_3 :off); Stage 2 (M :off, D_1 :off, D_2 :on, D_3 :on); Stage 3 (M :off, D_1 :off, D_2 :off, D_3 :on); Stage 4 (M :off, D_1 :off, D_2 :off, D_3 :off). All ideal concerning waveforms (v_{C_P} , v_{C_S} , i_L , i_{L_m}) are shown in Fig. 2.

Moreover, the dynamical model of AHPFC converter will be constructed by using the AM-TTS-DS methodology. Since the inductors L and L_m operating under DCM, it implies that $i_L(0) = i_L(T_S) = 0$ and $i_{L_m}(0) = i_{L_m}(T_S) = 0$. Therefore, all states of the converter are obtained as

$$\begin{cases} C_P \frac{d\langle v_{C_P}(t) \rangle_{T_S}}{dt} = \langle i_{C_P}(t) \rangle_{T_S} \\ C_S \frac{d\langle v_{C_S}(t) \rangle_{T_S}}{dt} = \langle i_{C_S}(t) \rangle_{T_S}, \end{cases}$$

where the symbol $\langle \cdot \rangle_{T_S}$ stands for the average function during one switching period T_S . From Fig. 2, the average function of all storage components are given as: $\langle v_L \rangle_{T_S} = \frac{1}{T_S}(d_1T_S\langle V_g \rangle_{T_S} - d_2T_S\langle v_{C_P} \rangle_{T_S})$, $\langle v_{L_m} \rangle_{T_S} = \frac{1}{T_S}(d_1T_S(\langle V_g \rangle_{T_S} + \langle v_{C_P} \rangle_{T_S}) - n(d_2 + d_3)T_S\langle v_{C_S} \rangle_{T_S})$, $\langle i_{C_P} \rangle_{T_S} = \frac{1}{T_S}(d_1^2T_S\frac{\langle V_g \rangle_{T_S} + \langle v_{C_P} \rangle_{T_S}}{2L_m} + (d_2T_S)^2\frac{\langle v_{C_P} \rangle_{T_S}}{2L})$, $\langle i_{C_S} \rangle_{T_S} = \frac{1}{T_S}(-(d_1 + d_2 + d_3 + d_4)T_S\frac{\langle v_{C_S} \rangle_{T_S}}{R} + (d_2 + d_3)^2T_S\frac{n^2\langle v_{C_S} \rangle_{T_S}}{2L_m})$.

Based on the voltage-seconds balance law, the average voltage of inductors $\langle v_L \rangle_{T_S}$ and $\langle v_{L_m} \rangle_{T_S}$ are equal to zero. Thus, the equations of v_L and v_{L_m} can be used to find the relationship of duty d_1 with d_2 , d_3 and d_4 as follows:

$$\begin{aligned} d_2 &= \frac{\langle V_g \rangle_{T_S}}{\langle v_{C_P} \rangle_{T_S}} d_1 \\ d_3 &= \left(\frac{\langle V_g \rangle_{T_S} + \langle v_{C_P} \rangle_{T_S}}{n\langle v_{C_S} \rangle_{T_S}} - \frac{\langle V_g \rangle_{T_S}}{\langle v_{C_P} \rangle_{T_S}} \right) d_1 \\ d_4 &= 1 - d_1 - d_2 - d_3 = 1 - \left(1 + \frac{\langle V_g \rangle_{T_S} + \langle v_{C_P} \rangle_{T_S}}{n\langle v_{C_S} \rangle_{T_S}} \right) d_1. \end{aligned} \quad (1)$$

The state equations of the converter are expressed as

$$\begin{aligned} C_P \frac{d\langle v_{C_P} \rangle_{T_S}}{dt} &= d_1^2 \frac{\langle V_g \rangle_{T_S} + \langle v_{C_P} \rangle_{T_S}}{2L_m} + (d_2^2 T_S) \frac{\langle v_{C_P} \rangle_{T_S}}{2L} \\ C_S \frac{d\langle v_{C_S} \rangle_{T_S}}{dt} &= -(d_1 + d_2 + d_3 + d_4) \frac{\langle v_{C_S} \rangle_{T_S}}{R} \\ &\quad + (d_2 + d_3)^2 \frac{n^2 \langle v_{C_S} \rangle_{T_S}}{2L_m}. \end{aligned} \quad (2)$$

Due to the switching frequency, 100 kHz is faster than the haversine frequency, 120 Hz. The input voltage V_g can be assumed as a constant value ($\langle V_g \rangle_{T_S} = V_g$) during switching period T_S . Furthermore, we substitute (1) into (2) and consider the $V_g(t) = |V_m \sin(\omega t)|$ during haversine period T_L . After combing the faster variable's affection on the slower variable, the average dynamics of the isolated AHPFC converter are derived as follows:

$$\begin{aligned} \frac{d\mathbf{v}_{C_P}}{dt} &= \frac{d_1^2(t)T_S}{2C_P} \left(\frac{V_m^2}{2L\mathbf{v}_{C_P}} - \frac{2V_m}{\pi L_m} - \frac{\mathbf{v}_{C_P}}{L_m} \right) \\ \frac{d\mathbf{v}_{C_S}}{dt} &= \frac{d_1^2(t)T_S}{2L_m C_S \mathbf{v}_{C_S}} \left(\frac{V_m^2}{2} + \frac{4V_m \mathbf{v}_{C_P}}{\pi} + \mathbf{v}_{C_P}^2 \right) - \frac{\mathbf{v}_{C_S}}{R}, \end{aligned} \quad (3)$$

where $\mathbf{v}_{C_P} = \langle \langle v_{C_P} \rangle_{T_S} \rangle_{T_L}$, $\mathbf{v}_{C_S} = \langle \langle v_{C_S} \rangle_{T_S} \rangle_{T_L}$ and the duty ratio $d_1(t)$ is a control input. The equation (3) is a nonlinear system since the control-input vector is two state-dependent, e.g., the terms of multiplying $d_1^2(t)$ by $\mathbf{v}_{C_P}(t)$ and dividing it by $\mathbf{v}_{C_S}(t)$, etc.

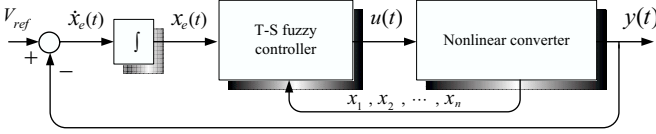


Fig. 3. Sketched diagram of integral T-S fuzzy control.

3. INTEGRAL T-S FUZZY REGULATOR

In this section, the proposed integral T-S fuzzy controller for the isolated AHPFC converter is described as the following five steps.

3.1 Integral-Type Control Design

Consider a general nonlinear system for the dynamic model (3) as follows:

$$\begin{aligned} \dot{x}_p(t) &= f(x_p(t)) + g(x_p(t))u(t) + \eta \\ y(t) &= h(x_p(t)) + l(x_p(t))u(t), \end{aligned} \quad (4)$$

where $x_p \in R^n$, $u \in R^c$, $y \in R^m$ are the state, the input, and the output vectors, respectively; and η is a constant term. The conceptual diagram of the integral T-S fuzzy control is depicted in Fig. 3. Here, control input $u(t)$ represents the duty cycle $d_1(t)$; V_{ref} is a constant reference; and $y(t)$ denotes the output voltage $\mathbf{v}_{CS}(t)$ for AHPFC converter system. We want to design an integral T-S fuzzy controller such that $y(t) \rightarrow V_{ref}$ as $t \rightarrow \infty$.

For achieving zero steady-state regulation error, the integral-type controller is robust to unmodelled uncertainty and exogenous disturbance. To account for the integral of output tracking error, we add a new state variable as $x_e = \int (V_{ref} - y(t))dt$, which results in the error dynamic equation $\dot{x}_e = V_{ref} - y(t)$. Therefore, from the model (3), the augmented dynamics of the isolated AHPFC converter is formed as follows:

$$\begin{aligned} \frac{dx_1}{dt} &= \frac{1}{C_S} \left(\frac{d_1^2 T_S}{2L_m x_1} \left(\frac{V_m^2}{2} + \frac{4V_m x_2}{\pi} + x_2^2 \right) - \frac{x_1}{R} \right) \\ \frac{dx_2}{dt} &= \frac{1}{C_P} \left(\frac{d_1^2 T_S}{2} \left(\frac{V_m^2}{2L x_2} - \frac{2V_m}{\pi L_m} - \frac{x_2}{L_m} \right) \right) \\ \frac{dx_3}{dt} &= V_{ref} - x_1, \end{aligned} \quad (5)$$

where $x_1 = \mathbf{v}_{CS}$, $x_2 = \mathbf{v}_{CP}$, and $x_3 = x_e$.

3.2 Coordinate Translation to Operation Point

The output regulation objective will be realized by stabilizing the system at an equilibrium state, which produces $\mathbf{v}_{CS}(t) = V_{ref}$. First, we must find \bar{x}_p and \bar{u} that are equilibrium points of the state x_p and control input u , respectively. For this purpose, let the right-hand side of the system (5) to be zero, we can obtain the equilibrium points as follows:

$$\begin{aligned} \bar{x}_1 &= V_{ref} \\ \bar{x}_2 &= \left(\sqrt{\frac{1}{\pi^2} + \frac{L_m}{2L}} - \frac{1}{\pi} \right) V_m \\ \bar{d}_1 &= \frac{V_{ref}}{\left(\sqrt{\frac{RT_S}{2L_m} \left(\frac{1}{2} \left(1 + \frac{L_m}{L} \right) + \frac{2}{\pi} \left(\sqrt{\frac{1}{\pi^2} + \frac{L_m}{2L}} - \frac{1}{\pi} \right) \right)} \right) V_m}. \end{aligned} \quad (6)$$

Second, let $x_1 = \tilde{x}_1 + \bar{x}_1$, $x_2 = \tilde{x}_2 + \bar{x}_2$, $x_3 = \tilde{x}_3 + \bar{x}_3$ and $d_1 = \tilde{d}_1 + \bar{d}_1$. As a designed parameter introduced by the integral control, the equilibrium point $\bar{x}_3 = \bar{x}_e$ will be determined later. After substituting (6) into (5), we obtain the following small signal model.

$$\begin{aligned} \dot{\tilde{x}}_1 &= \frac{1}{C_S} \left(\frac{(\tilde{d}_1 + \bar{d}_1)^2 T_S}{2L_m(\tilde{x}_1 + \bar{x}_1)} \left(\frac{V_m^2}{2} + \frac{4V_m x_2}{\pi} + (\tilde{x}_2 + \bar{x}_2)^2 \right) - \frac{x_1}{R} \right) \\ \dot{\tilde{x}}_2 &= \frac{1}{C_P} \left(\frac{(\tilde{d}_1 + \bar{d}_1)^2 T_S}{2} \left(\frac{V_m^2}{2L(\tilde{x}_2 + \bar{x}_2)} - \frac{2V_m}{\pi L_m} - \frac{x_2}{L_m} \right) \right) \\ \dot{\tilde{x}}_3 &= V_{ref} - (\tilde{x}_1 + \bar{x}_1) \end{aligned}$$

Note that in order to simplify the above dynamical equations, we neglect some higher-order terms (very small value). Therefore, the simplified model of the AHPFC converter can be obtained as follows:

$$\begin{aligned} \begin{bmatrix} \dot{\tilde{x}}_1 \\ \dot{\tilde{x}}_2 \\ \dot{\tilde{x}}_3 \end{bmatrix} &= \begin{bmatrix} \Psi & \frac{\bar{d}_1^2 T_S}{2\pi L_m C_S \bar{x}_1} (4V_m + 2\pi \bar{x}_2) & 0 \\ 0 & -\frac{\bar{d}_1^2 T_S}{2C_P} \left(\frac{1}{L_m} + \frac{V_m^2}{2L \bar{x}_2^2} \right) & 0 \\ -1 & 0 & 0 \end{bmatrix} \begin{bmatrix} \tilde{x}_1 \\ \tilde{x}_2 \\ \tilde{x}_3 \end{bmatrix} \\ &+ \begin{bmatrix} \frac{\bar{d}_1 T_S}{\pi L_m C_S \bar{x}_1} \Theta - \frac{\bar{d}_1 T_S}{\pi L_m C_S \bar{x}_1^2} \theta \tilde{x}_1 \\ \frac{\bar{d}_1 T_S}{C_P} \left(\frac{V_m^2}{2L \bar{x}_2} - \frac{2V_m}{\pi L_m} - \frac{\bar{x}_2}{L_m} - \left(\frac{1}{L_m} + \frac{V_m^2}{2L \bar{x}_2^2} \right) \tilde{x}_2 \right) \\ 0 \end{bmatrix} \tilde{d}_1, \end{aligned} \quad (7)$$

where $\theta = 0.5\pi V_m^2 + 4V_m \bar{x}_2 + \pi \bar{x}_2^2$, $\Theta = \theta + (4V_m + 2\pi \bar{x}_2) \bar{x}_2$ and $\Psi = -\frac{1}{C_S} \left(\frac{1}{R} + \frac{\bar{d}_1^2 T_S}{2\pi L_m \bar{x}_1^2} \Theta \right)$. Then, we must deal with the nonlinear characteristics of the converter.

3.3 Establish T-S Fuzzy Modelling System

According to the modelling approach, the dynamic system (7) with nonlinear terms can be exactly represented by T-S fuzzy model as the following rules:

$$\begin{aligned} \text{Plant Rule } i &: \text{IF } \tilde{x}_1(t) \text{ is } F_{1i} \text{ and } \tilde{x}_2(t) \text{ is } F_{2i} \text{ THEN} \\ \dot{\tilde{x}}(t) &= A_i \tilde{x}(t) + B_i \tilde{d}_1(t), \quad i = 1, 2, 3, 4, \end{aligned}$$

where $\tilde{x}(t) = [\tilde{x}_1(t) \ \tilde{x}_2(t) \ \tilde{x}_3(t)]^T$; $F_{1i}, F_{2i} (i=1, 2, 3, 4)$ are fuzzy sets. Moreover, let $\phi_1 = 0.5\pi V_m^2 + 4V_m \bar{x}_2 + \pi \bar{x}_2^2 + (4V_m + 2\pi \bar{x}_2) \mathcal{L}$, $\Phi_1 = \frac{1}{R} + \frac{\bar{d}_1^2 T_S}{2\pi L_m \bar{x}_1^2} \phi_1$; and $\phi_2 = 0.5\pi V_m^2 + 4V_m \bar{x}_2 + \pi \bar{x}_2^2 - (4V_m + 2\pi \bar{x}_2) \mathcal{L}$, $\Phi_2 = \frac{1}{R} + \frac{\bar{d}_1^2 T_S}{2\pi L_m \bar{x}_1^2} \phi_2$. We can obtain the linear subsystems' matrices as follows:

$$\begin{aligned} A_1 = A_2 &= \begin{bmatrix} -\frac{1}{C_S} \Phi_1 & \frac{\bar{d}_1^2 T_S}{2\pi L_m C_S \bar{x}_1} (4V_m + 2\pi \bar{x}_2) & 0 \\ 0 & -\frac{\bar{d}_1^2 T_S}{2C_P} \left(\frac{1}{L_m} + \frac{V_m^2}{2L \bar{x}_2^2} \right) & 0 \\ -1 & 0 & 0 \end{bmatrix}, \\ A_3 = A_4 &= \begin{bmatrix} -\frac{1}{C_S} \Phi_2 & \frac{\bar{d}_1^2 T_S}{2\pi L_m C_S \bar{x}_1} (4V_m + 2\pi \bar{x}_2) & 0 \\ 0 & -\frac{\bar{d}_1^2 T_S}{2C_P} \left(\frac{1}{L_m} + \frac{V_m^2}{2L \bar{x}_2^2} \right) & 0 \\ -1 & 0 & 0 \end{bmatrix}, \end{aligned}$$

$$B_1 = \left[\begin{array}{c} \frac{\bar{d}_1 T_S}{\pi L_m C_S \bar{x}_1} \phi_1 - \frac{\bar{d}_1 T_S}{\pi L_m C_S \bar{x}_1^2} (\theta \mathcal{K}) \\ \frac{\bar{d}_1 T_S}{C_P} \left(\frac{V_m^2}{2L\bar{x}_2} - \frac{2V_m}{\pi L_m} - \frac{\bar{x}_2}{L_m} - \left(\frac{1}{L_m} + \frac{V_m^2}{2L\bar{x}_2^2} \right) \mathcal{L} \right) \\ 0 \end{array} \right],$$

$$B_2 = \left[\begin{array}{c} \frac{\bar{d}_1 T_S}{\pi L_m C_S \bar{x}_1} \phi_1 + \frac{\bar{d}_1 T_S}{\pi L_m C_S \bar{x}_1^2} (\theta \mathcal{K}) \\ \frac{\bar{d}_1 T_S}{C_P} \left(\frac{V_m^2}{2L\bar{x}_2} - \frac{2V_m}{\pi L_m} - \frac{\bar{x}_2}{L_m} - \left(\frac{1}{L_m} + \frac{V_m^2}{2L\bar{x}_2^2} \right) \mathcal{L} \right) \\ 0 \end{array} \right],$$

$$B_3 = \left[\begin{array}{c} \frac{\bar{d}_1 T_S}{\pi L_m C_S \bar{x}_1} \phi_2 - \frac{\bar{d}_1 T_S}{\pi L_m C_S \bar{x}_1^2} (\theta \mathcal{K}) \\ \frac{\bar{d}_1 T_S}{C_P} \left(\frac{V_m^2}{2L\bar{x}_2} - \frac{2V_m}{\pi L_m} - \frac{\bar{x}_2}{L_m} + \left(\frac{1}{L_m} + \frac{V_m^2}{2L\bar{x}_2^2} \right) \mathcal{L} \right) \\ 0 \end{array} \right],$$

$$B_4 = \left[\begin{array}{c} \frac{\bar{d}_1 T_S}{\pi L_m C_S \bar{x}_1} \phi_2 + \frac{\bar{d}_1 T_S}{\pi L_m C_S \bar{x}_1^2} (\theta \mathcal{K}) \\ \frac{\bar{d}_1 T_S}{C_P} \left(\frac{V_m^2}{2L\bar{x}_2} - \frac{2V_m}{\pi L_m} - \frac{\bar{x}_2}{L_m} + \left(\frac{1}{L_m} + \frac{V_m^2}{2L\bar{x}_2^2} \right) \mathcal{L} \right) \\ 0 \end{array} \right],$$

where \mathcal{K} and \mathcal{L} are constant values denoting the interval that \tilde{x}_1 and \tilde{x}_2 lies within, i.e., $\tilde{x}_1 \in \{-\mathcal{K}, \mathcal{K}\}$ and $\tilde{x}_2 \in \{-\mathcal{L}, \mathcal{L}\}$. The grades of membership of $\tilde{x}(t)$ in the fuzzy set F_{ji} ($j = 1, 2$) are defined as: $M_{F_{11}}(\tilde{x}_1) = M_{F_{12}}(\tilde{x}_1) = \frac{1}{2}(1 + \frac{\tilde{x}_1}{\mathcal{K}})$; $M_{F_{13}}(\tilde{x}_1) = M_{F_{14}}(\tilde{x}_1) = \frac{1}{2}(1 - \frac{\tilde{x}_1}{\mathcal{K}})$; $M_{F_{21}}(\tilde{x}_2) = M_{F_{23}}(\tilde{x}_2) = \frac{1}{2}(1 + \frac{\tilde{x}_2}{\mathcal{L}})$; $M_{F_{22}}(\tilde{x}_2) = M_{F_{24}}(\tilde{x}_2) = \frac{1}{2}(1 - \frac{\tilde{x}_2}{\mathcal{L}})$. Consequently, the fuzzy plant model for the error signal $\tilde{x}(t)$ is inferred as follows:

$$\dot{\tilde{x}}(t) = \sum_{i=1}^4 \mu_i(\tilde{x}(t))(A_i \tilde{x}(t) + B_i \tilde{d}_1(t)), \quad (8)$$

where the $\mu_i(\tilde{x})$ are normalized weighting functions depended on \tilde{x}_1 and \tilde{x}_2 . Note that $\sum_{i=1}^4 \mu_i(\tilde{x}(t)) = 1$ for all t , and the $\mu_i(\tilde{x}) \geq 0$ can be defined as follows:

$$\mu_1(\tilde{x}) = M_{F_{11}}(\tilde{x}_1)M_{F_{21}}(\tilde{x}_2); \mu_2(\tilde{x}) = M_{F_{12}}(\tilde{x}_1)M_{F_{22}}(\tilde{x}_2);$$

$$\mu_3(\tilde{x}) = M_{F_{13}}(\tilde{x}_1)M_{F_{23}}(\tilde{x}_2); \mu_4(\tilde{x}) = M_{F_{14}}(\tilde{x}_1)M_{F_{24}}(\tilde{x}_2).$$

To design $\tilde{d}_1(t)$, the concept of parallel distributed compensation (PDC) is applied. The i th rule of the control input is described as follows:

$$\text{Control Rule } i : \text{ IF } \tilde{x}_1(t) \text{ is } F_{1i} \text{ and } \tilde{x}_2(t) \text{ is } F_{2i} \text{ THEN}$$

$$\tilde{d}_1(t) = -K_i \tilde{x}(t), \quad i = 1, 2, 3, 4.$$

The fuzzy controller in the consequent part is inferred as follows:

$$\tilde{d}_1(t) = - \sum_{i=1}^4 \mu_i(\tilde{x}) K_i \tilde{x}(t). \quad (9)$$

By substituting (9) into (8), the closed-loop system can be represented as

$$\dot{\tilde{x}}(t) = \sum_{i=1}^4 \sum_{j=1}^4 \mu_i \mu_j (A_i - B_i K_j) \tilde{x}(t)$$

$$= \sum_{i=1}^4 \sum_{j=1}^4 \mu_i \mu_j G_{ij} \tilde{x}(t). \quad (10)$$

3.4 Stability Analysis and Controller Gains

Feedback gains K_i and system stability are simultaneously presented. Choose the Lyapunov function $V(\tilde{x}(t)) = \tilde{x}^\top(t) P \tilde{x}(t) > 0$, where P is a symmetric positive definite matrix. Taking time derivative of $V(\tilde{x})$ along with (10), it yields

$$\dot{V}(\tilde{x}(t)) = \sum_{i=1}^4 \sum_{j=1}^4 \mu_i \mu_j \tilde{x}^\top(t) (G_{ij}^\top P + P G_{ij}) \tilde{x}(t).$$

If P satisfies $G_{ij}^\top P + P G_{ij} < 0$ or a little bit of stronger condition:

$$G_{ij}^\top P + P G_{ij} + DPD < 0, \quad (11)$$

where D is a diagonal positive definite matrix, then we can obtain $V(\tilde{x}(t)) \leq V(0) e^{-\frac{\lambda_{\min}(DPD)}{\alpha \lambda_{\max}(P)} t}$, where $\lambda_{\min}(M)$ and $\lambda_{\max}(M)$ denote the minimal and maximal eigenvalue of matrix M , respectively. Therefore, $\|\tilde{x}\|^2 \leq \frac{V(0)}{\lambda_{\min}(P)} e^{-\frac{\lambda_{\min}(DPD)}{\alpha \lambda_{\max}(P)} t}$ is concluded.

As to the inequality, after pre multiplying and post multiplying $X = P^{-1}$, we can obtain

$$(A - BK_i)X + X(A^\top - K_i^\top B^\top) + (DX)^\top X^{-1}DX < 0.$$

Letting $M_i = K_i X$ and applying Schur's complement, (11) can be equivalently written as the following LMIs:

$$\begin{bmatrix} A_i X + X A_i^\top & -B_i M_j - M_j^\top B_i^\top & X D^\top \\ DX & & -X \end{bmatrix} < 0. \quad (12)$$

Therefore, if there exist a common symmetric positive definite matrix $X = P^{-1}$ such that the LMIs in (12) are feasible, then the system (8) can be exponentially stabilized via the PDC fuzzy controller (9) with $K_i = M_i X^{-1}$. The K_i and X can be together obtained by solving (12) via Matlab's LMI toolbox.

3.5 Accomplishment of Integral T-S Fuzzy Controller

Because the plant has two state variables with one output term, the control input of the system (3) will be taken as

$$d_1 = \tilde{d}_1 + \bar{d}_1$$

$$= - \sum_{i=1}^4 \mu_i(\tilde{x}) \left([K_{i1} \ K_{i2}] \begin{bmatrix} x_1 - \bar{x}_1 \\ x_2 - \bar{x}_2 \end{bmatrix} + K_{i3}(x_e - \bar{x}_e) \right) + \bar{d}_1.$$

The controller gains (K_{i1}, K_{i2}, K_{i3}) can be obtained once there exists an $X > 0$ such that (12) is feasible. When applied to the AHPFC converter, we notice that after transient response the variation of $\mu_i(\tilde{x})$ is often kept within a small region. Thus, it is natural to let

$$\bar{x}_e = \left(\sum_{i=1}^4 \mu_i(\tilde{x}) K_{i3} \right)^{-1} \left(\bar{d}_1 - \sum_{i=1}^4 \mu_i(\tilde{x}) [K_{i1} \ K_{i2}] \begin{bmatrix} \bar{x}_1 \\ \bar{x}_2 \end{bmatrix} \right),$$

Table 1. Parameters of AHPFC converter

Parameters	Value and Unit
Peak voltage, V_m	156 V
Storage inductance, L	167.7 μ H
Exciting inductance, L_m	990 μ H
Storage capacitance, C_P	470 μ F
Output capacitance, C_S	10000 μ F
Maximum load resistance, R_{full}	12 Ω
Minimum load resistance, R_{light}	18 Ω
Switching period, T_S	10 μ sec
Haversine's period, T_L	$\frac{1}{120}$ sec
Turns ratio of transformer, n	12 turn

and regard it as the equilibrium point of x_e . The flexibility of designing \bar{x}_e as above equation is related to the robustness of integral-type control. Consequently, the control input can be represented as

$$d_1(t) = - \sum_{i=1}^4 \mu_i(\tilde{x})(K_i x(t)), \quad (13)$$

where $K_i = [K_{i1} \ K_{i2} \ K_{i3}]$ and $x = [x_1 \ x_2 \ x_3]^T$.

4. NUMERICAL SIMULATION

In this section, the proposed integral T-S fuzzy regulation is verified by numerical simulations successfully.

According to Table 1 and equation (6), the DC operating points of the states and control input can be obtained as $\bar{x}_1 = \bar{v}_{C_S} = 12$ V, $\bar{x}_2 = \bar{v}_{C_P} = 222.9208$ V, $\bar{d}_1 = 0.2116$. To keep the inductor's current under DCM and consider the capacitor's ripple affection, we appropriately choose $-\mathcal{K} = -1$, $\mathcal{K} = 1$, $-\mathcal{L} = -1$ and $\mathcal{L} = 1$ for application to the isolated AHPFC converter in this design. Based on LMIs (12) and let decay rate $D = \text{diag}\{20.93, 1.18, 9.09\}$, the control gains are obtained below:

$$\begin{aligned} K_{11} = K_{21} = K_{31} = K_{41} &= 0.451869, \\ K_{12} = K_{22} = K_{32} = K_{42} &= 0.000647, \\ K_{13} = K_{23} = K_{33} = K_{43} &= -40.24111. \end{aligned} \quad (14)$$

Thanks to this nice property, the control law (13) is further reduced to $d_1(t) = -K_1 x_1 - K_2 x_2 - K_3 x_3$, which is a linear one.

To verify the performance of the isolated AHPFC converter with the integral T-S fuzzy controller, the variations of the load are tested. The results simulated by Matlab are shown in Fig. 4, where including the state (x_1, x_2) , the integral error state (x_e) and control input (duty ratio) responses of the converter, which is subjected to the load R changed from 18 Ω to 12 Ω at 0.1 s and then changed from 12 Ω to 18 Ω at 0.2 s.

5. CONTROL CIRCUITS AND EXPERIMENT

According to (13) and getting LMI-based gains (14), we can implement the integral T-S fuzzy controller of the isolated AHPFC converter by using electrical circuits that contain operational amplifiers, resistors and variable resistors. The control input is realized in Figs. 5 ~ 6. Fig. 5

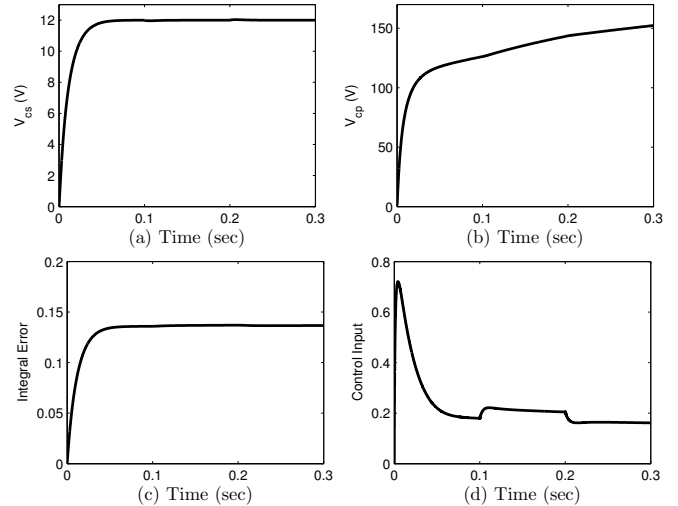


Fig. 4. (a) Output voltage v_{C_S} , (b) capacitor's voltage v_{C_P} , (c) integral error state x_e , and (d) control input of the converter, for the R changed: 18 $\Omega \rightarrow 12 \Omega \rightarrow 18 \Omega$.

shows the integral error circuit of the designed controller, where the V_{ref} is set to be 12 V and the $v_o(t)$ denotes the practical output voltage. In Fig. 6, the $x_1(t)$, $x_2(t)$ and $x_3(t)$ are the system's three states that are multiplied by relative feedback gains to form the linear control part of the controller. Note that the membership functions circuit and the nonlinear control part of the controller have been omitted.

The experimental results are shown in Fig. 7. Fig. 7(a) and (b) respectively show the output voltage transient responses in AC mode for the converter, which is subjected to the load variations changed from 18 Ω to 12 Ω at 0.1 s and back to 18 Ω at 0.2 s.

As well as the simulation results, the oscillograms exhibit the perfect robustness to the variations of the load and the output always maintain at 12 V. Specially, these have nice performances such as short settling time, small overshoot, zero steady state error and fast transient response.

6. CONCLUSION

In this paper, the integral T-S fuzzy controller has prevented the bulk capacitor from crossing high voltage stress while the load is at a light level for the AC-DC isolated AHPFC converter. The proposed control strategy can exactly model the converters and deal with its heavy nonlinear characters. The local feedback gains are obtained by solving a set of LMIs. The perfect large-signal stability and transient variations have been simulated by Matlab. The experimental results reveal the satisfactory output voltage responses and the excellent input current shape for power factor correction. Compared to the PI controller, the proposed method can cope with the inherently nonlinear character for the converters in a nonlinear method. Besides, the stability analysis of the traditional fuzzy approach has been improved by the suggested control scheme.

REFERENCES

- J.-L. Lin, M.-Z. Chang, and S.-P. Yang. Synthesis and analysis for a novel single-stage isolated high power factor correction converter. *IEEE Trans. Circuits and Systems I*, volume 52, no. 9, pages 1928–1939, Sept. 2005.
- H. Y. Kanaan, A. Marquis, and K. Al-Haddad. Small-signal modeling and linear control of a dual boost power factor correction circuit. *Proc. IEEE PESC'04*, pages 3127–3133, 2004.
- K. Viswanathan, R. Oruganti, and D. Srinivasan. Non-linear function controller: A simple alternative to fuzzy logic controller for a power electronic converter. *IEEE Trans. Ind. Electron.*, volume 52, no. 5, pages 1439–1448, Oct. 2005.
- P. Kirawanich and R. M. O'Connell. Fuzzy logic control of an active power line conditioner. *IEEE Trans. Power Electron.*, volume 19, no. 6, pages 1574–1585, Nov. 2004.
- K. Tanaka, T. Ikeda, and H. O. Wang. Fuzzy regulators and fuzzy observer: Relaxed stability conditions and LMI-based designs. *IEEE Trans. Fuzzy Syst.*, volume 6, no. 2, pages 250–265, May 2000.
- K.-Y. Lian, J.-J. Liou, and C.-Y. Huang. LMI-based integral fuzzy control of DC-DC converters. *IEEE Trans. Fuzzy Syst.*, volume 14, no. 1, pages 71–80, Feb. 2006.
- J. Sun and H. Grotstollen. Averaged modeling of switching power converters: Reformulation and theoretical basis. *Proc. IEEE PESC'92*, pages 1165–1172, 1992.

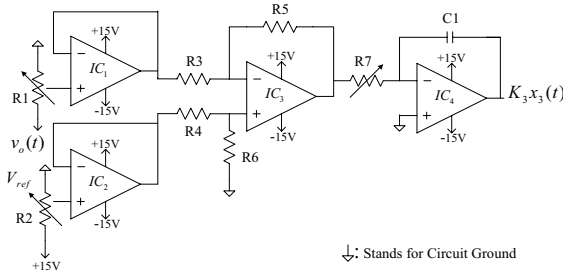


Fig. 5. Integral error circuit of the controller.

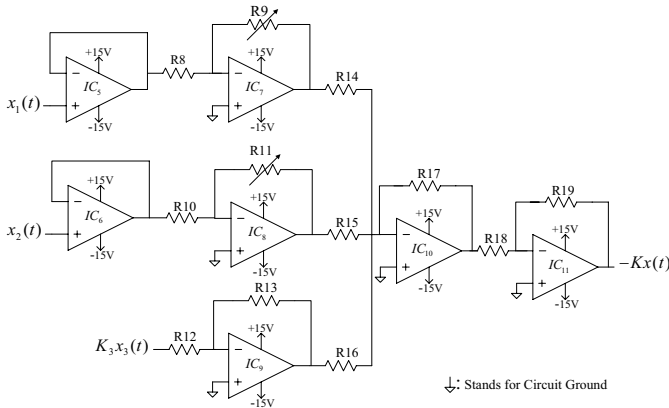


Fig. 6. Linear control circuit of the controller.

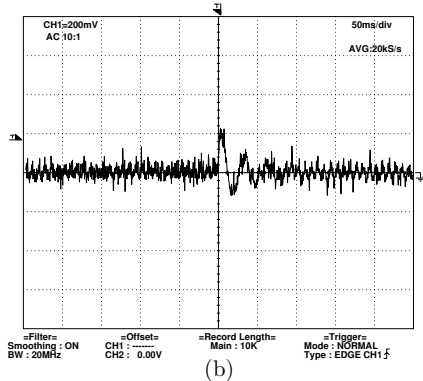
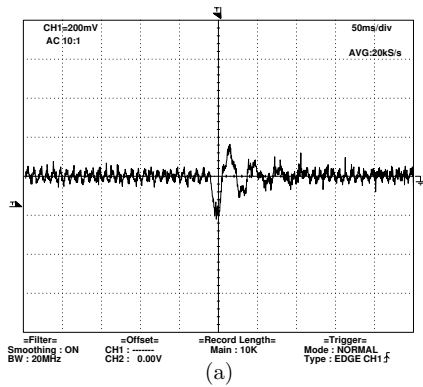


Fig. 7. Output voltage responses in AC mode, when the R changed: (a) $18 \Omega \rightarrow 12 \Omega$; (b) $12 \Omega \rightarrow 18 \Omega$.